

## Supplementary Information

# Structure and Properties of Composite Films Formed by Cellulose Nanocrystals and Latex Nanoparticles

Héloïse Thérien-Aubin, Ariella Lukach, Natalie Pitch, Eugenia Kumacheva

### S1. Experimental

**Materials.** All chemicals were purchased from Sigma-Aldrich, unless specified. The surfactant sodium dodecyl sulfate (SDS) and cetylammonium bromide (CTAB), the initiators potassium persulfate (KPS) and 2-2-azo-*bis*(2-methylpropionamidine) dihydrochloride (V-50) (Acros), as well as the fluorescently labeled monomer 9-vinyl anthracene (VA), were used as received. The monomers butyl acrylate (BuA) and ethyl methacrylate (EtMA) were purified by column filtration over aluminum oxide. A suspension of CNCs (obtained by acid hydrolysis of wood pulp) was purchased from the USDA Forest Product Laboratory (U.S.A.).

**Synthesis of negatively-charged 150 nm-diameter latex particles.** Latex particles were synthesized in a semi-continuous “seed-and-feed” process. First, 3.5mL of EtMA was emulsified in 55 mL of deionized water containing 12.5 mg of SDS. The suspension was heated to 80 °C and purged with N<sub>2</sub> for 30 min. Under stirring provided by a mechanical stirrer at 200 rpm, a solution of 60 mg of KPS in 5 mL of water was injected to the suspension at a rate of 0.5 mL/min. After 1 h of polymerization, a solution of 100 mg of VA in 30 mL of EtMA and a solution of 40 mg of KPS and 37.5 mg of SDS in 25 mL of water were injected to the polymerization flask at a rate of 3 and 2.5 mL/min, respectively. After 20 h, the polymerization was stopped, and the latex dispersion was purified by dialysis against deionized water for one week, the water was changed every day.

***Synthesis of positively-charged 150 nm-diameter latex particles.*** Latex particles were synthesized in a semi-continuous “seed-and-feed” process. First, 3.5mL of EtMA was emulsified in 55 mL of deionized water containing 25 mg of CTAB. The suspension was heated to 80 °C and purged with N<sub>2</sub> for 30 min. Under stirring provided by a mechanical stirrer at 200 rpm, a solution of 60 mg of V-50 in 5 mL of water was injected to the suspension at a rate of 0.5 mL/min. After 1 h of polymerization, a solution of 100 mg of VA in 15 mL of EtMA and a solution of 40 mg of V-50 and 75 mg of CTAB in 25 mL of water were injected to the polymerization flask at a rate of 1.5 and 2.5 mL/min, respectively. After 20 h, the polymerization was stopped, and the latex dispersion was purified by dialysis against deionized water for one week, the water was changed every day.

***Synthesis of positively-charged 50 nm-diameter latex particles.*** Latex particles were synthesized in a semi-continuous “seed-and-feed” process. First, 3.5mL of EtMA was emulsified in 55 mL of deionized water containing 50 mg of CTAB. The suspension was heated to 80 °C and purged with N<sub>2</sub> for 30 min. Under stirring provided by a mechanical stirrer at 200 rpm, a solution of 60 mg of V-50 in 5 mL of water was injected to the suspension at a rate of 0.5 mL/min. After 1 h of polymerization, a solution of 50 mg of VA in 10 mL of EtMA and a solution of 40 mg of V-50 and 150 mg of CTAB in 25 mL of water were injected to the polymerization flask at a rate of 1 and 2.5 mL/min, respectively. After 20 h, the polymerization was stopped, and the latex dispersion was purified by dialysis against deionized water for one week, the water was changed every day.

***Synthesis of negatively-charged 50 nm-diameter latex particles.*** Latex particles were synthesized in a continuous process, in which 50 mg of VA was dissolved in 7.5 mL of EtMA. The monomer mixture was emulsified in 55 mL of deionized water containing 1 g of SDS. The suspension was heated to 80 °C and purged with N<sub>2</sub> for 30 min. Under stirring provided by a mechanical stirrer at 200 rpm, a solution of 60 mg of KPS in 5 mL of water was injected to the suspension at a rate of 0.5 mL/min. The solution was then

stirred at 80°C for 2 h. The latex dispersion was purified by dialysis against deionized water for one week, the water was changed every day.

**Characterization.** The hydrodynamic dimensions and electrokinetic potentials ( $\zeta$ -potential) of the CNC and latex particles were analyzed with a Zetasizer Nano-ZS-Zen3600 (Malvern). The glass transition of the latex particles was measured by differential scanning calorimetry on a DSC2900 (TA Instruments) using a heating rate of 10 °C/min. A Cary-5000 spectrophotometer was used to record the extinction spectra of the films. Circular dichroism spectra were recorded on a Jasco J-710 spectropolarimeter. Transmission electron microscopy (TEM) imaging of CNCs was performed on a Hitachi H-7000 microscope. Scanning electron microscopy (SEM) imaging of composite films and latex particles was performed on a Quanta FEG 250 environmental microscope. Polarized optical microscopy (POM) and fluorescence imaging ( $\lambda_{\text{ex}}=320-390$  nm,  $\lambda_{\text{em}} > 420$  nm) were performed using an Olympus BX51 microscope.

## S2. Characterization of the CNCs and the latex particles

**Size distribution of the CNCs.** Transmission Electron Microscopy (TEM) images of individual CNCs cast from the dilute CNCs suspension were used to characterize the CNC width and length (Figure S1). The analysis of 212 individual CNCs gave an average length and diameter of  $180 \pm 70$  and  $13 \pm 4$  nm, respectively.

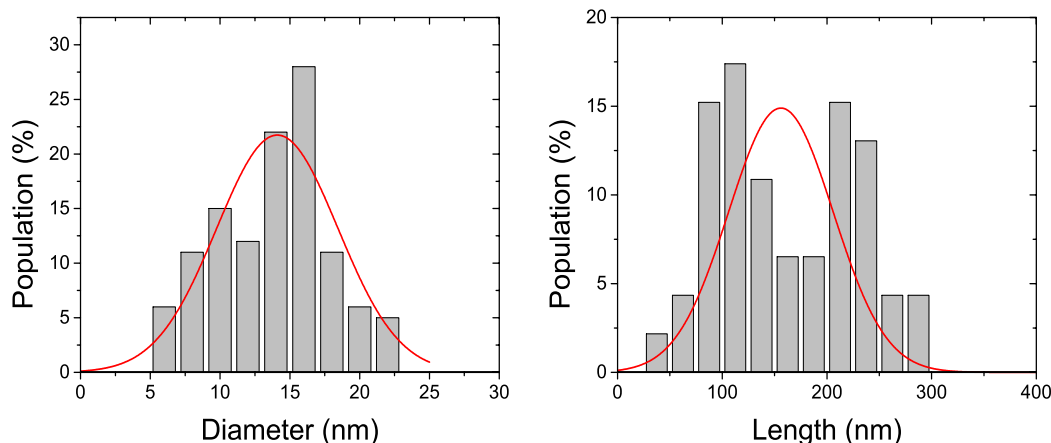


**Figure S1.** The distribution of CNC diameters (a) and lengths (b) measured by analyzing TEM images of 212 CNCs.

### Surface-charge and size distributions of latex particles and CNCs

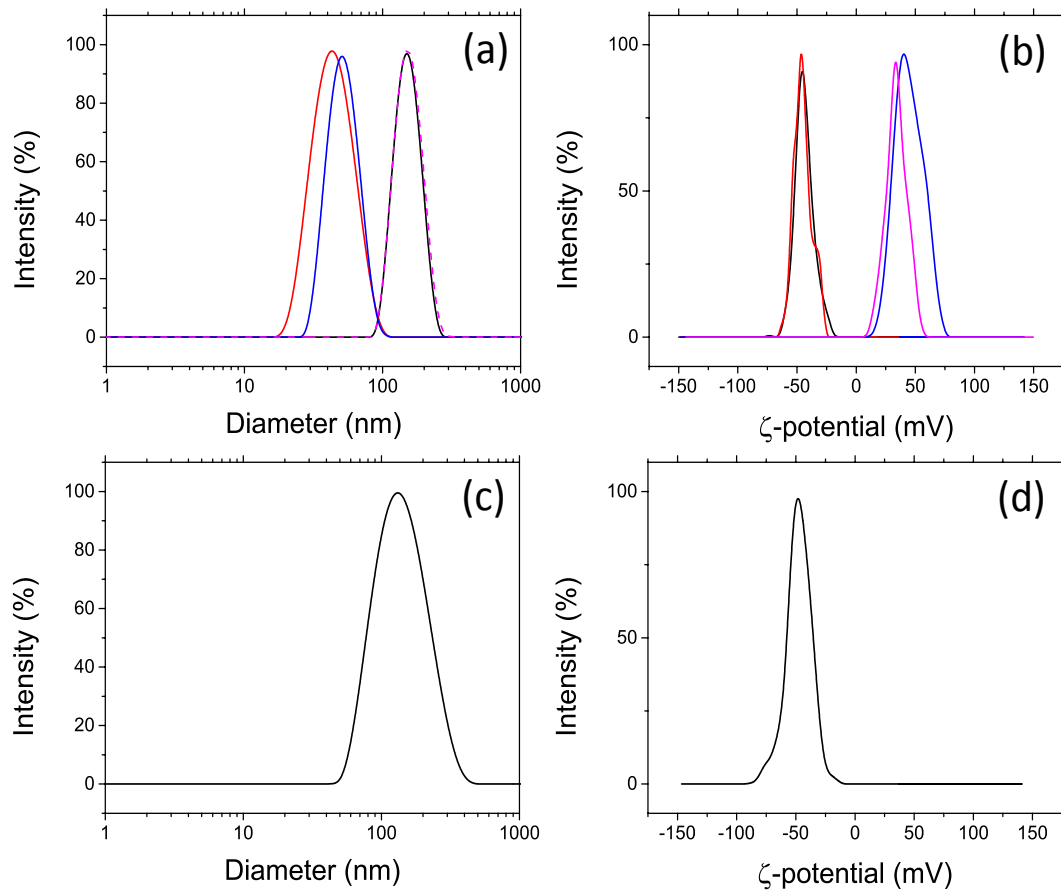


**Figure S2.** (a) Hydrodynamic diameter and (b) electrokinetic potential of EtMA150(-) (black lines), EtMA50(-) (red lines), EtMA150(+) (pink lines), and EtMA50(+) (blue lines). (c) Effective hydrodynamic diameter of CNCs and (d) Electrokinetic potential of CNCs.

**Characterization of fluorescence properties of dye-labeled latex particles**

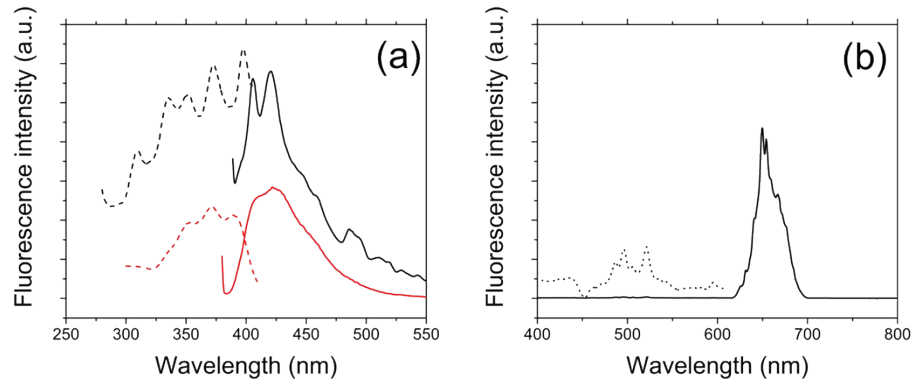


**Figure S3.** (a) Fluorescence spectra of EtMA150(−) (red lines) and EtMa150(+) (black lines) latex particles labeled with vinyl anthracene. Solid lines show emission spectra acquired at  $\lambda_{\text{ex}}=350$  nm. Dashed lines show excitation spectra recorded at  $\lambda_{\text{em}}=420$  nm.. (b) Autofluorescence of CNCs suspension.  $\lambda_{\text{ex}}=350$  nm;  $\lambda_{\text{em}}=400-800$  nm. The dotted line in (b) shows the spectrum multiplied by 25-folds.

### S3. Optical properties of CNC-latex composite films

In solid films, CNCs formed a chiral nematic structure, with a left-handed helical organization oriented perpendicularly to the plan of the film and reflecting left-handed circularly polarized light. This CNC organization led to a positive circular dichroism signal (Figure S4).

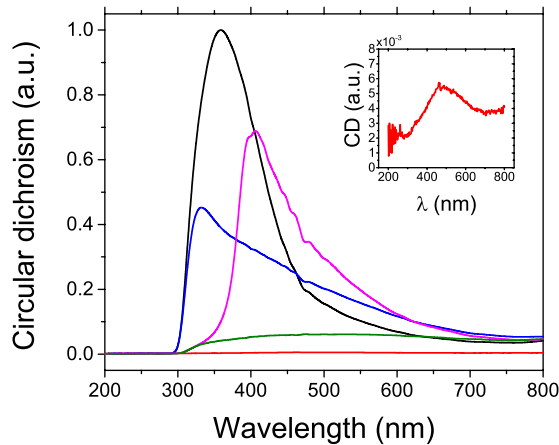


**Figure S4.** Circular dichroism properties of the composite films with  $C_{\text{latex}} = 25$  wt% containing EtMA50(−) (pink line), EtMA150(−) (blue line), EtMA50(+) (red line), and EtMA150(+) (green line) latex particles. The inset show a magnified view of the film made with EtMA150(+) latex particles. The spectrum of the latex-free CNC film is shown with a black line for comparison.

### S4. Viscosity of mixed CNC/latex NP suspensions

Upon addition of negatively-charged latex particles to the suspension of negatively-charged CNCs, a weak increase in viscosity was observed (Fig. S5a). In contrast, mixing of positively-charged latex particles with a suspension of CNCs led to strong increase in the viscosity of the CNC-latex suspension (Fig. S5b). The mixed CNC-latex suspensions of EtMA50(+) latex NPs were shear thinning and, in absence of shear, the suspension displayed gel-like properties.

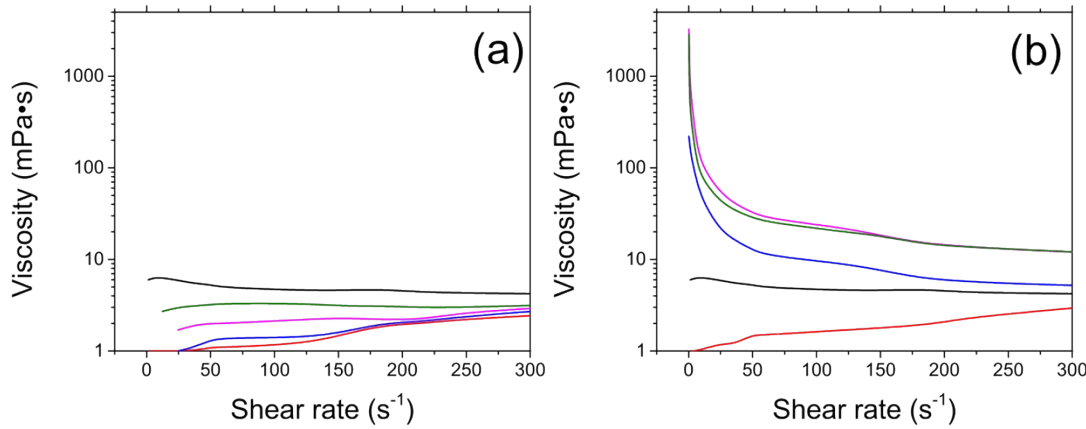


**Figure S5.** Viscosity of mixed 2.5 wt% suspension of CNCs and 50 nm-diameter EtMA50(−) (a) and EtMA50(+) (b). The fraction of latex NPs in the solid content was (black) 0%, (green) 25%, (pink) 50%, (blue) 75% and (red) 100%.

### S5. Phase separation in mixed CNC-latex suspensions

Mixed suspension of CNCs and latex NPs were prepared by mixing 1.5 mL of 2.5 wt% suspension of CNC and 0.5 mL of a 2.5 wt% suspension of latex NPs. After 3 day equilibration, images of the mixed suspensions were taken under white light and ultraviolet (UV) light illumination. Figure S6a shows the photographs of the phase-separated suspensions of CNC-latex, latex-free CNCs, and CNC-free latex suspensions under white light illumination. Figure S6b shows the same systems under UV light illumination. The latex-free CNCs suspension phase-separated into a chiral nematic phase (bottom layer) and an isotropic phase (top layer). Based on fluorescence, latex particles ((both EtMA50(−) and EtMA150(−)) partitioned in the CNC-rich (bottom layer) and CNC-poor (top layer) phases (Fig. S6 i and ii). However, phase separation between a chiral nematic phase and an isotropic phase was not observed in presence of EtMA50(+) and EtMA150(+) particles (Fig. S6 iii and iv). In this system CNCs and latex particles formed a gel-like precipitate.

Similarly, the phase separation between CNC-rich and CNC-poor phases is also visible in thin liquid films. After 3 days of equilibration in a capillary cell, the CNC-rich regions displayed birefringence when observed in polarized optical microscopy (POM). Figure S7a shows the POM images of the phase separated CNC-latex suspension. The CNC-rich phase form birefringent droplets displaying a typical fingerprint texture are

dispersed in a isotropic (black) CNC-poor phase. Fluorescence images (Fig. S7b) recorded in the same position in the sample shows that the fluorescently labeled latex NPs are partially excluded from the ordered domains.

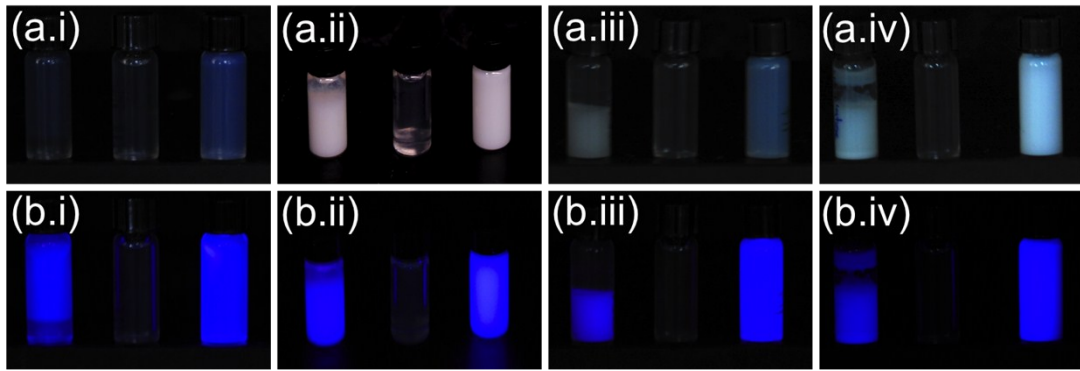


**Figure S6.** Macroscopic phase separation in the mixed CNC-latex suspension. The suspension was irradiated with (a) white light and (b) UV light at  $\lambda_{\text{exc}}=365$  nm. In (a) and (b) the left sample is CNC-latex suspension at  $C_{\text{latex}}=25\text{ \%}$ ; the middle sample is a latex-free CNC suspension ( $C_{\text{latex}}=0$ ) and the right sample is the CNC-free latex suspension ( $C_{\text{latex}}=100\text{ \%}$ ). The labels are: (i) EtMA50(−), (ii) EtMA150(−), (iii) EtMA50(+), and (iv) EtMA150(+) latex NPs.

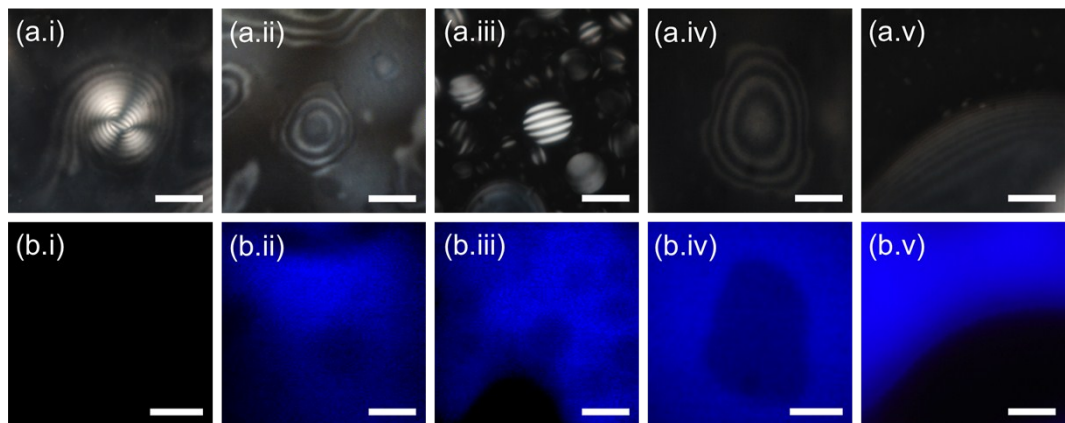


**Figure S7.** Polarized optical microscopy (top, labeled as a) and fluorescence microscopy images (bottom, labeled as b) of (i) Latex-free suspension and (ii-v) mixed suspension with  $C_{\text{latex}}= 25\text{wt\%}$ . (ii) EtMA50(−) NPs; (iii) EtMA50(+) NPs; (iv) EtMA150(−) NPs; (v) EtMA150(+) NPs. Scale bars are  $100\text{ }\mu\text{m}$ .

## S6. Polarized optical microscopy images of composite films

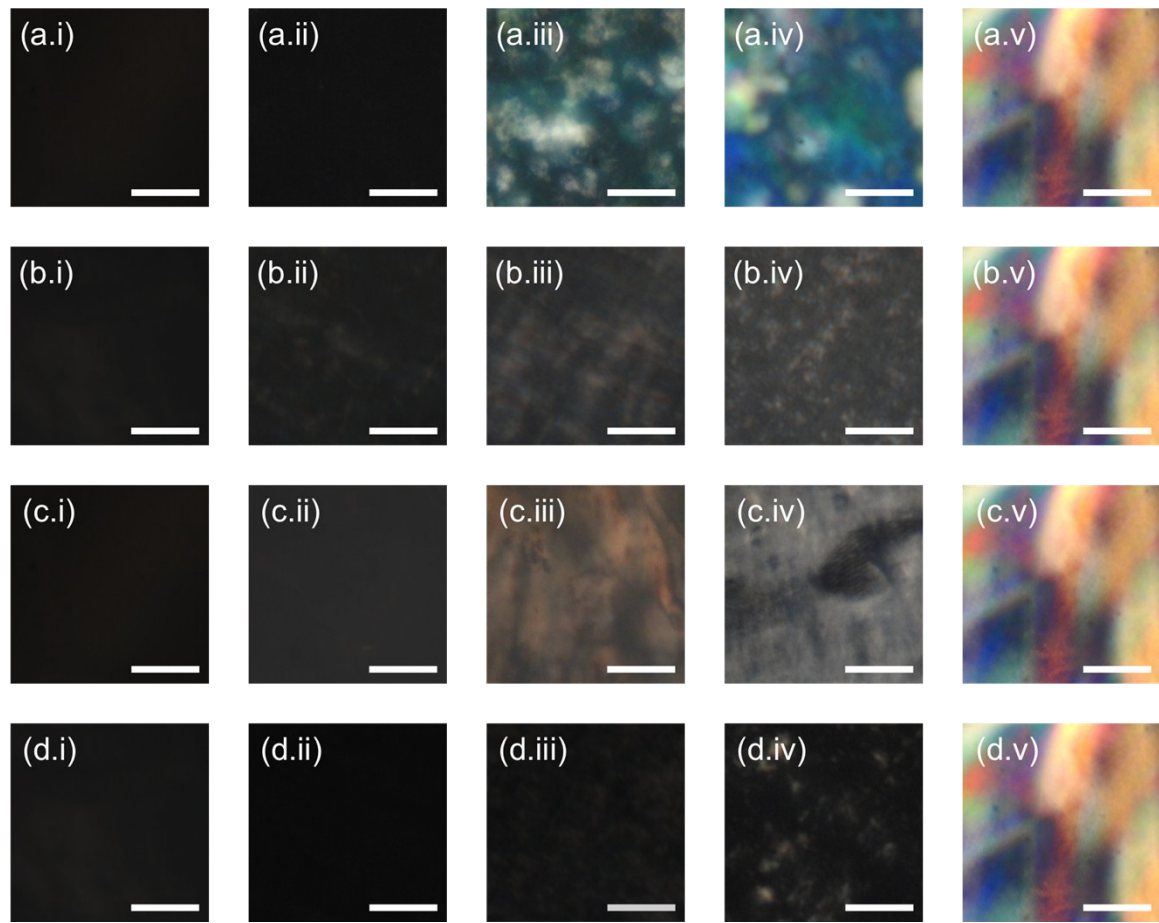


**Figure S8.** Polarized optical microscopy images of the composite CNC films containing (a) EtMA50(−); (b) EtMA50(+); (c) EtMA150(−); and (d) EtMA150(+) latex NPs at  $C_{\text{latex}}$  (wt %) of (i) 100; (ii) 75; (iii) 50; (iv) 25 and (v) 0. Scale bars are 50  $\mu\text{m}$

### S7. Fluorescence images of composite films

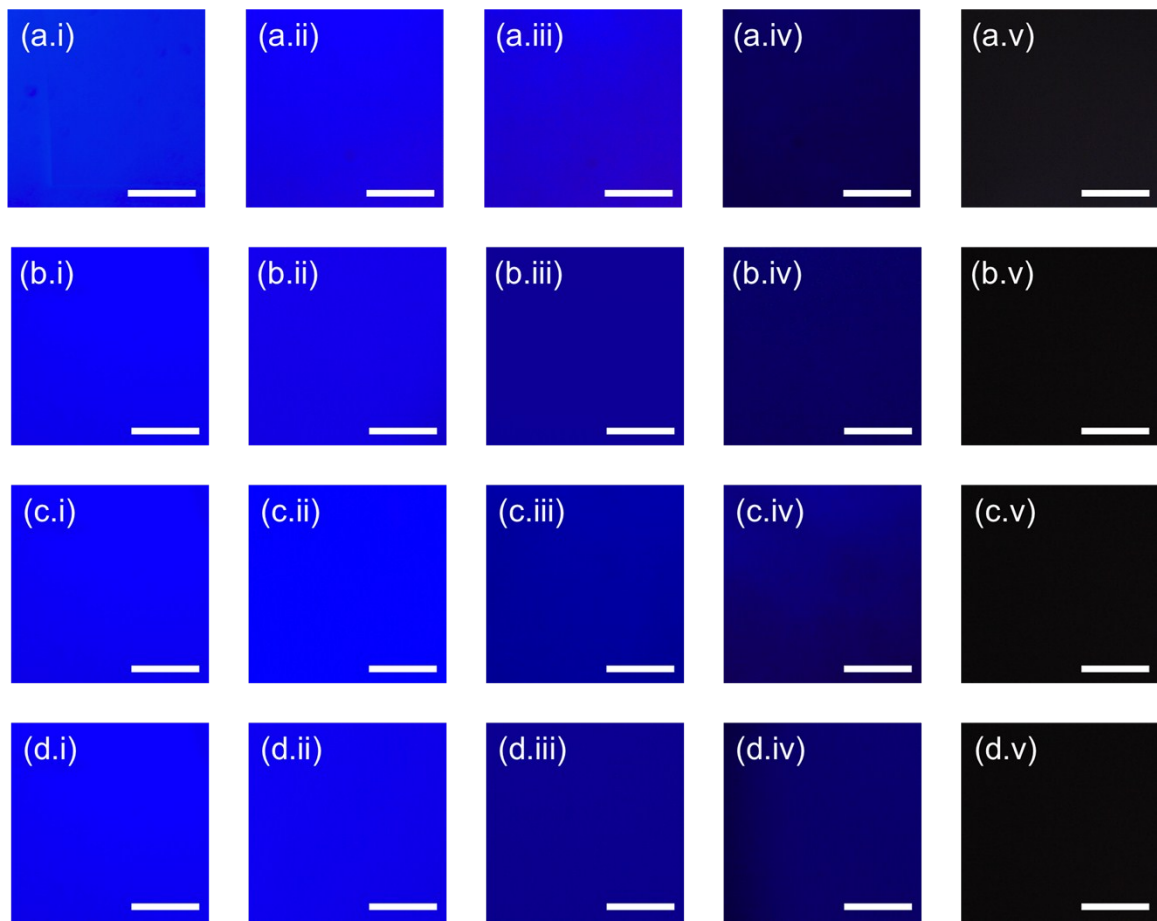


**Figure S9.** Fluorescence microscopy images of composite films of CNC and (a) EtMA50(−); (b) EtMA50(+); (c) EtMA150(−); (d) EtMA150(+) latex particles at  $C_{\text{latex}}$  (wt %) of (i) 100; (ii) 75; (iii) 50; (iv) 25 and (v) 0. Scale bars are 50  $\mu\text{m}$

## S8. Scanning electron microscopy images of composite films

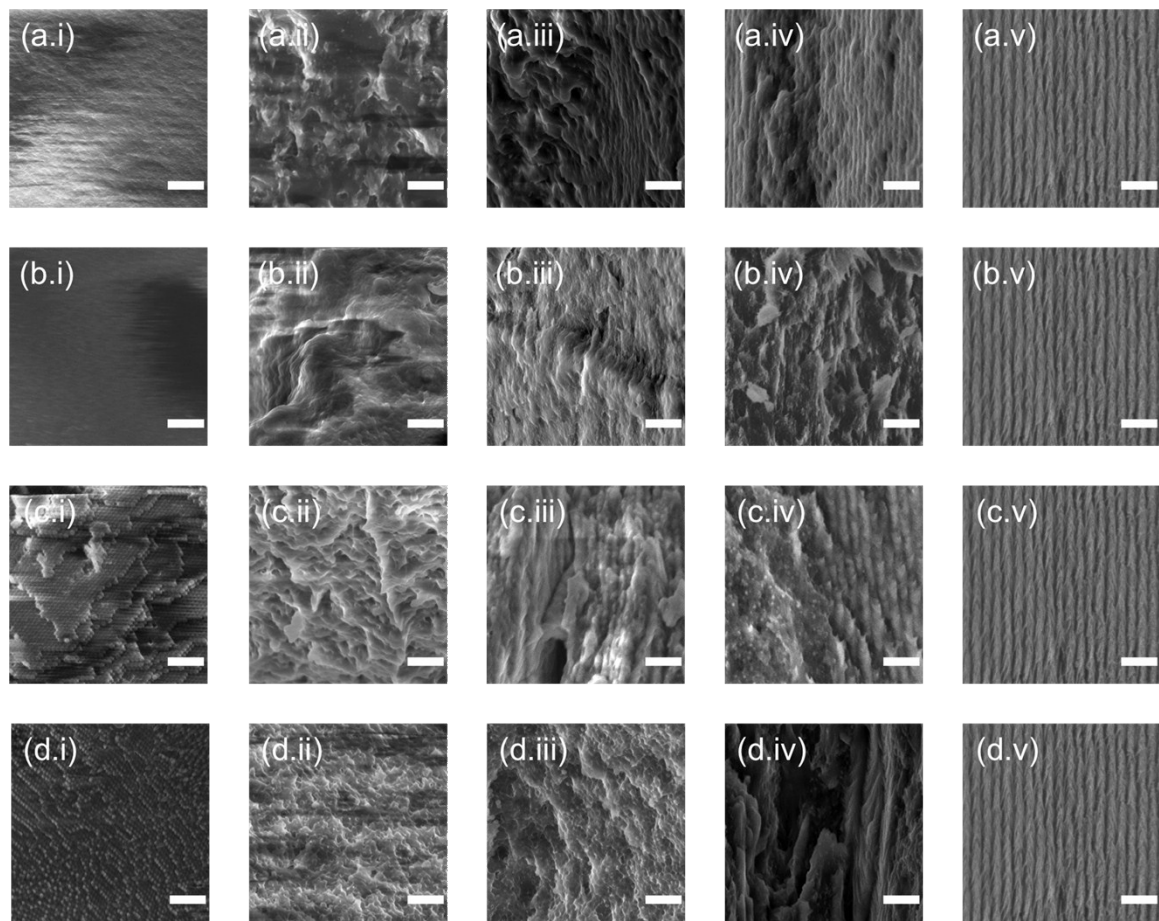


**Figure S10.** Scanning electron microscopy of the cross-sections of composite CNC films containing (a) EtMA50(−); (b) EtMA50(+); (c) EtMA150(−); and (d) EtMA150(+) latex particles at  $C_{\text{latex}}$  of (i) 100%; (ii) 75%; (iii) 50%; (iv) 25% and (v) 0%. Scale bars are 1  $\mu\text{m}$

## S9. Quantification of latex rich domains in the film

The fraction of latex-rich domains in the composite films (Figure S12a) was determined in the following manner:

1. A mask shown in Figure S11b was created by delimiting the regions covered by the N\* domains and the disordered latex-rich domains, in which
  - (i) the N\* domains were labeled with a blue color;
  - (ii) the disordered domains were labeled with a red color;
  - (iii) the areas of the image that were not part of the sample, e.g., solid support, air outside the samples) were labeled in black
2. The number of blue and red pixels in the image was measured using MATLAB.

The fraction of the surface covered with latex-rich domains was determined as

$$\% \text{ latex-rich domains} = \frac{nb_{red}}{nb_{blue} + nb_{red}},$$

where % latex-rich domains is the fraction of the surface of the cross-section occupied by the latex-rich domains,  $nb_{red}$  the number of red pixels and  $nb_{blue}$  the number of blue pixels in the images. The analysis of 10 cross-sectional images give an average fraction of latex-rich domains of  $19 \pm 10 \%$  for films made of CNCs and 25 wt% of EtMA150(–) NPs and  $12 \pm 10 \%$  for films made of CNCs and 25 wt% of EtMA50(–) NPs.

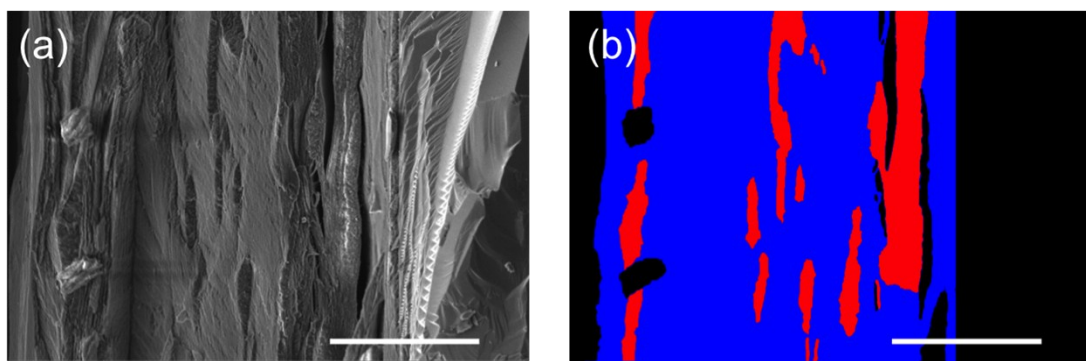


**Figure S11.** Analysis of the area covered by latex NP-rich domains in the CNC-latex composite film with EtMA150(–) ( $C_{\text{latex}}=25 \text{ wt\%}$ ). (a) Original SEM image of the cross-section of the composite film and (b) mask. Scale bar is  $10 \mu\text{m}$ . In the mask, the red regions represent the disordered region, the blue regions the ordered domains and the black the discarded area (air, void or solid support)

### S11. Inclusion of latex NPs in the N\* phase

High magnification SEM images of the cross-sections of the composite films showed the inclusion of the latex NPs within the CNC-rich chiral nematic region of the film. (Fig. S12).

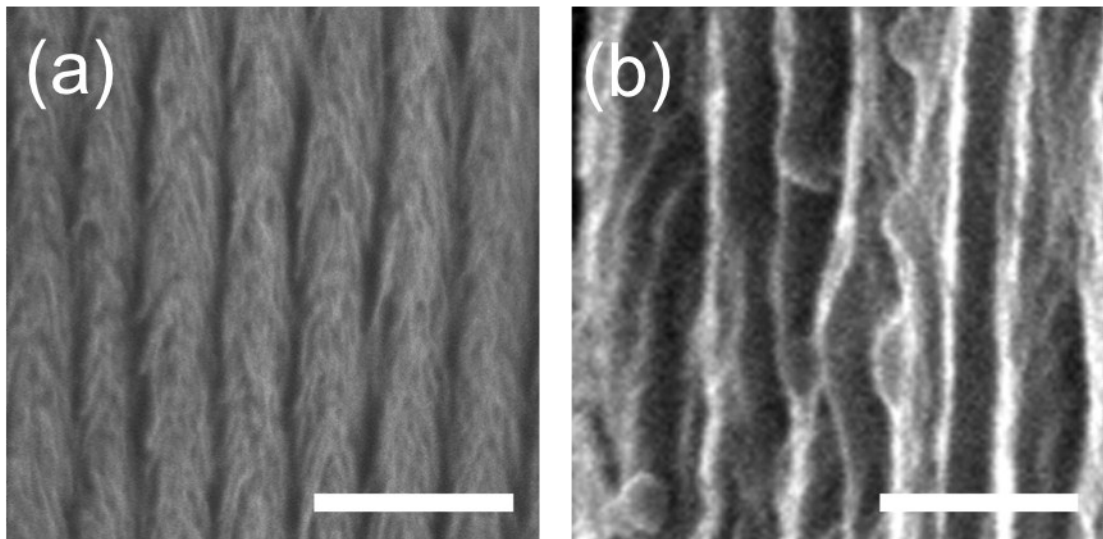


**Figure S12.** SEM images of the cross-section of (a) a latex-free CNC film and (b) composite CNC film containing EtMA150(-) latex particles at  $C_{\text{latex}}=25 \text{ wt\%}$ . Scale bars are 500 nm.

### S11. Effect thermal treatment on latex films and latex-free CNC films

In films formed by drying a dispersion poly(ethyl methacrylate) latex NPs at 25°C or at 25°C (under  $T_g$ ) with subsequent annealing at 75 °C (above  $T_g$ ), the NPs packed in a face-centered close-packed (fcc) lattice (Fig. S13a and b, respectively). When these films were prepared directly at 75 °C, no fcc structures were observed (Fig. S13c).

The structure of latex-free CNC films was also considerably influenced by the drying conditions: rapid water evaporation lead to the formation of less dense films with a larger N\* pitch.<sup>1</sup> The CNC films obtained at 25°C displayed a well-ordered N\* regions (Fig. S13d), giving rise to a narrow stop-band at  $380\pm20 \text{ nm}$ . After annealing the latex-free CNC film at 75 °C for 18 h, the N\* structure was preserved (Fig. S13e) and a similar

stop-band is measured. The CNC films obtained directly at 75 °C exhibited a broader and red-shifted stop-band, compared to CNC films prepared at 25°C, indicative of a less ordered structure (Fig. S13e).

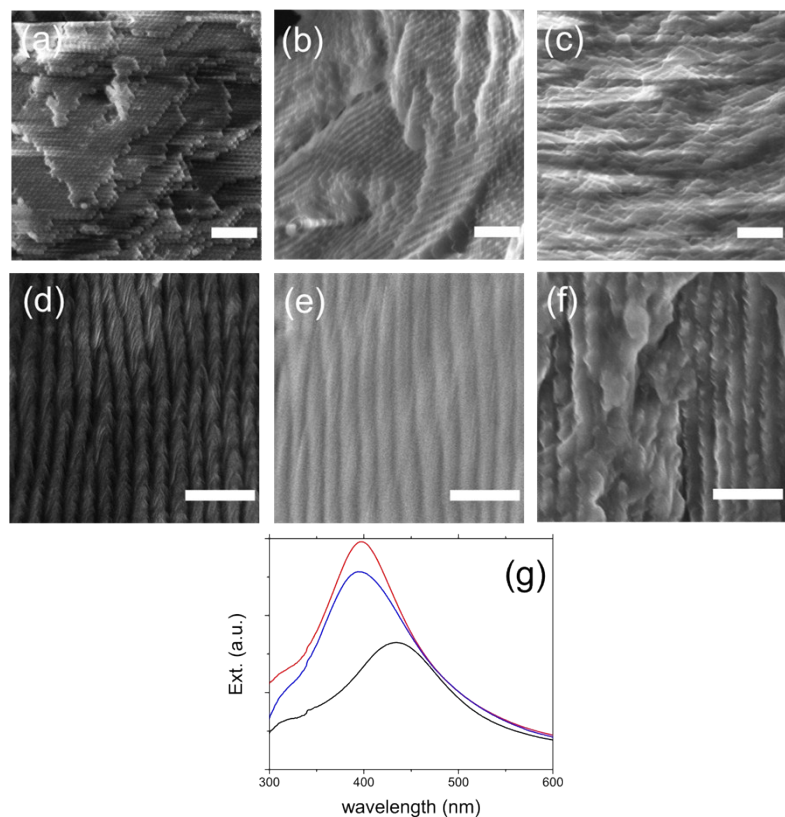


**Figure S13.** SEM images of (a-c) CNC-free latex films and (d-f) latex-free CNC films, formed at 25 °C (a,d), formed at 25 °C and subsequently, annealed at 75 °C (b,e) and formed at 75 °C (c,f). Scale bars are 1  $\mu$ m. (g) Extinction spectra of latex-free CNC films formed at 25 °C (blue spectrum), formed at 75°C (black spectrum) and formed at 25 °C and subsequently, annealed at 75 °C (red spectrum).

## References

(1) Beck, S.; Bouchard, J.; Chauve, G.; Berry, R. *Cellulose* **2013**, *20*, 1401-1411.